Journal of Computer Engineering
ISSN 10003428

Original Research Article
Vol 12, Issue 6, 2023 | ISSN: 1000-3428

A Comparative Evaluation of Cloning Strategies for Aerodynamic Compressor Design via Throughflow Analysis

Julian R. Thompson and Emily J. Lee
Department of Aerospace Engineering, University of Cambridge, Cambridge CB2 1PZ, UK

Abstract

Due to their high complexity, aero engine development is a time-consuming and cost-intensive process. Therefore, pre-developed proven aerodynamic and geometric compressor information is often used as starting point and transferred to new compressor designs. In the present paper, a new approach for aerodynamic cloning of an already existing compressor flow to a new compressor geometry by use of a streamline curvature based Throughflow solver is presented. Parameterized compressor quantities are automatically modified with the help of optimization strategies, and the resulting compressor aerodynamics are compared to a reference design in each iteration step. The target is to minimize the discrepancy between reference design and new design regarding essential flow parameters like de Haller number, Mach number etc., and thereby to reproduce the aerodynamic image of the reference design. Thus, already collected experience from existing compressor flow fields can be used to reduce costs for developing as well as testing of new compressor configurations. Conducted investigations show a notable acceleration of the design process in comparison to former strategies starting from scratch while achieving an acceptable compliance of aerodynamic parameters.

Indexed keywords: Computer Engineering, Advanced Computing, Technology, Open Access

Article History: Received: 27 February 2023 | Accepted: 12 May 2023 | Published: 01 June 2023

INTRODUCTION

Increasing requirements concerning performance and reliability as well as constantly shortened development cycles force the aerospace industry to exploit more and more design process automation and optimization strategies. They enable an efficient solution of increasingly complex problems with often contradicting design objectives and a large number of design parameters and constraints. For aero engine development, these kind of strategies are especially used for aerodynamic design of respective components such as compressor, combustor, and turbine (Keskin, 2007).

In general, the complexity of aero engines requires an independent development of components in cascaded design cycles with increasing degree of fidelity (Pöhlmann, 2015). The first design phase with least fidelity is represented by a performance calculation. Here, essential parameters such as temperatures and pressures are defined with the help of thermodynamic cycle calculations. The resulting values then serve as boundaries for the subsequent individual component design processes based on higher-fidelity models.

A more detailed compressor design is conducted by firstly using 1D Meanline calculation, followed by 2D Throughflow evaluation and blade design up to final 3D CFD calculations (Pöhlmann, 2015). The latter allows for a detailed evaluation of 3D flow phenomena while requiring a comparatively high amount of time, which is why this tool is not considered here. Although computational effort for Meanline or Throughflow evaluation is low, the required design time increases enormously if optimization strategies are involved, especially if design tools of different fidelity are coupled as shown by Pöhlmann (2015). This complicates industrial application and makes reliable performance investigations between different design strategies or different optimization algorithms difficult.

To overcome these challenges, the present paper introduces an alternative automated design approach based on Throughflow calculations. To obtain a suitable design, the aerodynamic properties of a known and approved compressor configuration are cloned instead of searching for a set of optimal compressor designs from scratch by use of multi-objective optimization as applied by Rühle (2013).

THROUGHFLOW-BASED COMPRESSOR DESIGN

As already pointed out, the Meanline design process is typically evaluated as a first design step to define annulus geometry and feasible flow properties for aerofoils along the annulus mid-height line like exit flow angles or stage pressure ratios. This information then serves as a basis for the subsequent Throughflow design process, where a streamline curvature method is used to determine flow information in radial direction of the

How to cite: Julian R. Thompson and Emily J. Lee (2023). A Comparative Evaluation of Cloning Strategies for Aerodynamic Compressor Design via Throughflow Analysis. Journal of Computer Engineering, 12(6), 69–78. DOI: https://doi.org/10.5281/zenodo.19349270

meridional plane. At the end of this design step, radial distributions for all aerodynamic parameters are defined which can be used to design suitable aerofoil shapes for each blade row.

Flow parameters with significant impact on stable engine operation are the stator exit flow angle and the stage pressure ratio, which is why they should be selected carefully. For example, the radial adaption of the stator exit flow angle influences the formation of the axial velocity profile having a high impact on the subsequent rotor station and its efficiency. Adjustment of a stator guide vane and definition of a special pre-whirl in front of a rotor may prevent flow separation near the hub section. Front stages are of particular concern because of transonic Mach numbers (Cumpsty, 2004). To guarantee a safe partial load engine operation and a uniform inflow to rear compressor stages, the stage pressure ratio of the front stages (typically first three stages) must be processed properly.

Existing Throughflow-based design processes use optimization strategies (Rühle and Bestle, 2010) to find completely new compressor configurations with regard to objectives like compressor efficiency η and surge margin SM while meeting essential aerodynamic criteria such as limited stage loading, flow velocity, and suction side delay. By summarizing them as inequality constraints $\mathbf{h}_T \leq \mathbf{0}$, a representative multi-criterion Throughflow compressor optimization problem may be described as

$$\max_{\mathbf{p}_T \in P_T} \begin{bmatrix} \eta \\ SM \end{bmatrix} \quad where \quad P_T = \{\mathbf{p}_T \in \mathbb{R}^m | \mathbf{h}_T \leq \mathbf{0}\} \tag{1}$$

The design vector $\mathbf{p}_T$ summarizes various design parameters to be modified by the optimizer. In the present case, exit flow angles α_E and stage pressure ratios π for each compressor stage are adjusted. To reduce the number of design parameters, to smooth radial distributions, and to make the optimization strategy more flexible and independent from geometry settings like number of stages, smooth parameterisation strategies are used (Hinz, 2012). Thereby free-form geometries maintain almost the same design freedom, which is why they are also applied here.

Especially B-splines (Schönberg, 1946) are utilized which are composed of piecewise polynomial functions and allow for local adaption of the spline parts. According to
(Piegl and Tiller, 1997), planar curves are parameterized as

$$\begin{bmatrix} x(t) \\ y(t) \end{bmatrix} = \sum_{i=0}^{n} N_{i,p}(t)\, \boldsymbol{P}_i \tag{2}$$

for the x and y coordinates, with B-spline basis polynomials $N_{i,p}(t)$ of degree p, number $(n+1)$ of control points $\boldsymbol{P}_i$, and curve parameter $t \in [0,1]$.

Figure 1a shows exemplarily the parameter reduction for a continuous point cloud by use of a B-spline curve. Instead of varying all tip annulus points individually, the points are fitted and replaced by a B-spline (red curve). The spline control point coordinates (red diamonds) may serve as new design parameters which are adjusted by the optimizer. By modifying the control points, a variation of the spline curve shape may be induced, which finally affects the original annulus points because both B-spline curve and annulus points are correlated (Hinz, 2012).

Instead of fitting the original points and modifying the resulting spline control points, an additional perturbation spline may be used alternatively. In this strategy, splines define radial deviation values Δr which are then added to the position of the original points. This directly changes the point cloud or curve outline by moving the control points of the perturbation spline. Figure 1 shows the effect of such a perturbation spline (Fig. 1b) on a point graph. The red vertical lines attached to the hub contour points in Fig. 1a illustrate the shifting of the original points resulting from perturbation. Due to the normalized size, perturbation splines are independent of the dimensions of the reference geometry. Furthermore, the number of control points of the perturbation spline may be chosen independently and kept constant, being ideal for an automated design process. In contrast, the number of control points for a fitted curve depends on the fitting quality and can be

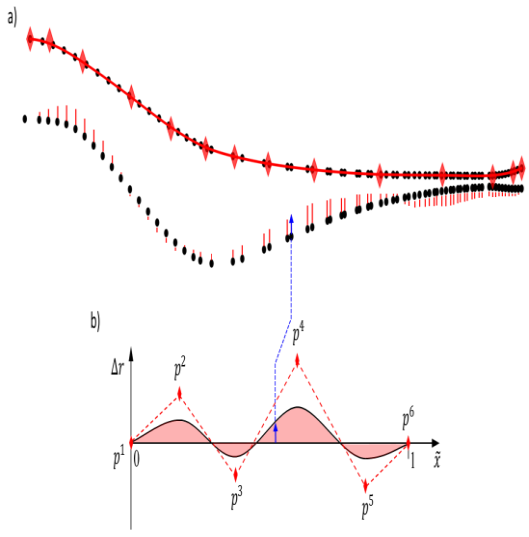

Figure 1 Modification of annulus point

changed by modifying the reference contour.

In the present case, the radial distributions of stator exit flow angles are modified by superimposing constant Meanline values with perturbations for each compressor stage. There are several ways of shaping the radial profile: linearly, D-shape, and nonlinearly, while here only linear and nonlinear profiles are investigated.

The linear approach is the easiest way to manipulate the radial distribution of a flow parameter. According to Rühle (2013), the manipulation of e.g. the stator exit flow angle may be calculated as

$$\alpha_E^S(\tilde{x}, \tilde{r}) = \bar{\alpha}_E^S(\tilde{x}) + \Delta\bar{\alpha}_E^S(\tilde{x}) + \Delta\alpha'^S_E(\tilde{x}) \cdot (\tilde{r} - 0.5) \quad (3)$$

where $\bar{\alpha}_E^S(\tilde{x})$ is the flow angle at the radial midline given by the Meanline calculation, $\Delta\bar{\alpha}_E^S(\tilde{x})$ describes a constant offset value regarding this mean value, and $\Delta\alpha'^S_E(\tilde{x})$ is the slope from hub to casing. Figure 2 shows exemplarily the superimposing (3) and the resulting radial exit flow angle distribution at e.g. the stator exit position of stage five $\tilde{x}_5$. The dimensionless axial $\tilde{x}$ and radial $\tilde{r}$ coordinates are defined as

$$\tilde{x} = \frac{x - x^S_{E,1}}{x^S_{E,n_S-1} - x^S_{E,1}} \in [0,1] \quad (4)$$

$$\tilde{r} = \frac{r(x) - r_h(x)}{r_c(x) - r_h(x)} \in [0,1] \quad (5)$$

where $x_E^S{}_{,1}$ and $x_E^S{}_{,ns-1}$ describe the axial coordinates of the first and the second last stator stage (trailing edge

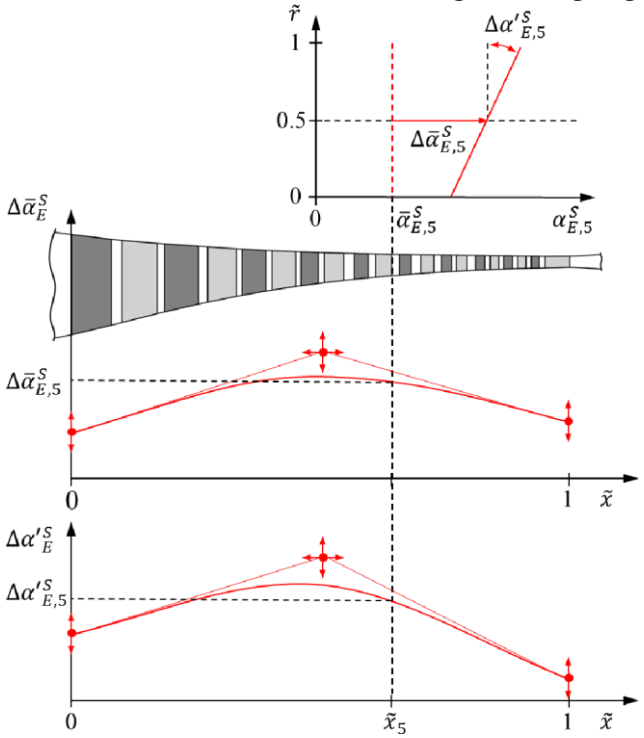

Figure 2 Modification of stator exit flow angle by use of perturbation splines

chosen to limit the design space. The first and last control points are fixed in axial direction, respectively, while the radial direction is free and can be varied together with the mid control point by the optimizer, where corresponding coordinates are part of design vector $\mathbf{p}_C$.

The presented parameterization does not involve the inlet guide vane (IGV), which is considered separately to prevent limitations due to the B-spline parameterization (Rühle, 2013). Similar to Eq. (3), the position, respectively), and r_h and r_c represent the radial coordinates for hub and casing. Here, the last compressor stage will not be considered in the design parameterisation, because an exit flow angle of zero is required for axial compressor configurations to guarantee a nearly swirl-free inflow into the combustion chamber.

The distributions for offset $\Delta\bar{\alpha}_E^S(\tilde{x})$ and slope $\Delta\alpha'^S_E(\tilde{x})$ are described by two perturbation splines

$$\begin{bmatrix} \tilde{x}(t) \\ \Delta\bar{\alpha}^S_E(t) \end{bmatrix} = \sum_{i=0}^{n} N_{i,p}(t)\, \boldsymbol{P}_i^{\Delta\bar{\alpha}^S_E}, \quad t \in [0,1] \quad (6)$$

$$\begin{bmatrix} \tilde{x}(t) \\ \Delta\alpha'^S_E(t) \end{bmatrix} = \sum_{i=0}^{n} N_{i,p}(t)\, \boldsymbol{P}_i^{\Delta\alpha'^S_E}, \quad t \in [0,1] \quad (7)$$

exemplarily shown in Fig. 2. For the present investigations$_S$, a constant number of three control points and is

radial exit flow angle distribution of the IGV is represented by

$$\alpha_E^{IGV}(\tilde{r}) = \bar{\alpha}_E^{IGV} + \Delta\bar{\alpha}_E^{IGV} + \Delta\alpha'^{IGV}_E(\tilde{r} - 0.5). \quad (8)$$

The linear distribution approach is rather stiff and inflexible for stage specific flow adjustments. Hence, Rühle (2013) developed a nonlinear distribution approach which is also investigated here. To get a nonlinear radial stator exit flow angle distribution, the linear term is exchanged by a nonlinear function $f^S(\tilde{x}, \tilde{r})$ for stators and
$f^{IGV}(\tilde{r})$ for the IGV resulting in the following equations:

$$\alpha_E^S(\tilde{x}, \tilde{r}) = \bar{\alpha}_E^S(\tilde{x}) + \Delta\bar{\alpha}_E^S(\tilde{x}) + \Delta\alpha'^S_E(\tilde{x}) \cdot (f^S(\tilde{x}, \tilde{r}) - 0.5), \quad (9)$$

$$\alpha_{EIGV}(\tilde{r}) = \bar{\alpha}_{EIGV} + \Delta\bar{\alpha}_{EIGV} + \Delta\alpha'_{IGVE}(f_{IGV}(\tilde{r}) - 0.5). \quad (10)$$

At hub and casing, the nonlinear functions $f^{IGV}(\tilde{r}) \in [0,1]$ and $f^S(\tilde{x}, \tilde{r}) \in [0,1]$ are set to minimum and maximum
values, i.e.,

$$f^{IGV,S}(\tilde{r} = 0) = 0, \quad (11)$$

$$f_{IGV,S}(\tilde{r} = 1) = 1. \quad (12)$$

Thereby, the exit flow angle values at hub and casing are fixed similar to the linear distribution, and a deviation from the linear distribution is only possible in between.

For the nonlinear function associated with the IGV, a quadratic B-spline curve with three control points is used. Equations (11) and (12) require a fixation of the first control point to [0,0] and the last one to [1,1], such that only one control point with two degrees of freedom (as part of design parameter $\mathbf{p}_C$) remains:

$$\begin{bmatrix} \tilde{r}(t) \\ f^{IGV}(t) \end{bmatrix} = \sum_{i=0}^{2} N_{i,2}(t) \boldsymbol{P}_i^{f^{IGV}}, \quad t \in [0,1] \quad . \tag{13}$$

To define the complete radial stator exit angle distribution for all stages, the function $f^S(\tilde{x}, \tilde{r})$ depends on two variables. For this purpose, a 2D parameterization strategy is no longer sufficient, which is why the problem formulation is extended to a 3D B-spline surface. In the present case, a quadratic B-spline surface with three control points in each of the directions t and u is chosen:

$$\begin{bmatrix} \tilde{x}(t,u) \\ \tilde{r}(t,u) \end{bmatrix} = \sum_{i=0}^{2}\sum_{j=0}^{2} N_{i,2}(t) N_{j,2}(u) \, \boldsymbol{P}_{i,j}^{f^S} \quad , \quad f^S(t, u) \tag{14}$$

$$\begin{bmatrix} t \\ u \end{bmatrix} \in [0,1]^2 .$$

Regarding all limitations, only nine design parameters remain to modify the surface (14).

The specific outflow of the fan section causes strong differences of the total pressure profile in radial direction. Especially the weak pressure profile near the hub section has a major impact on the core engine. The flow enters the swan neck duct and finally meets the compressor section, where a high flow deflection in the front stages near the hub section is necessary to compensate the weak pressure profile. This causes high losses during the compression process and leads to an unstable operation during partial load. To solve this problem, the stage pressure ratio of the first three compressor stages is reprocessed in addition to the exit flow angles to receive a strong hub profile. For the determination of a new pressure profile, an approach based on scaling is used. With the help of a B-spline surface, factors $\tilde{\pi}(\tilde{x}, \tilde{r})$ are defined and superimposed with the given Meanline values $\bar{\pi}(\tilde{x})$. In contrast to the stage pressure ratio, this is done by multiplication according to Rühle and Bestle (2010) resulting in

$$\pi(\tilde{x}, \tilde{r}) = \bar{\pi}(\tilde{x}) \cdot \tilde{\pi}(\tilde{x}, \tilde{r}) \, . \tag{15}$$

To make the strategy generic, the stage pressure ratios are referred to dimensionless axial $\tilde{x}$ and radial $\tilde{r}$ coordinates. The B-spline surface is built with 3 × 3 control points, which proved to be sufficient and necessary to adjust each stage individually:

$$\begin{bmatrix} \tilde{x}(t,u) \\ \tilde{r}(t,u) \\ \tilde{\pi}(t,u) \end{bmatrix} = \sum_{i=0}^{2}\sum_{j=0}^{2} N_{i,2}(t) N_{j,2}(u) \, \boldsymbol{P}_{i,j}^{\tilde{\pi}} \, , \begin{bmatrix} t \\ u \end{bmatrix} \in [0,1]^2. \tag{16}$$

Only the stage pressure ratios of the first three stages are modified. The design freedom of the nine surface control points for the pressure factor (16) results in eleven additional design parameters.

AERODYNAMIC CLONING

The introduced design parameters are the basis for the new cloning process described in the following. Instead of finding a best compressor aerodynamic by optimization, the goal is to clone the flow field of an already existing and proven compressor configuration to obtain a new compressor with changed geometry, number of stages etc., but similar aerodynamic behavior. This has the advantage that better estimates for the compressor behavior under modified operating conditions are obtained, since the new configuration is operating in an already validated working range. The process is inspired by cloning strategies used for compressor aerofoils as presented by Gräsel et al. (2004). From an industrial perspective, the design of a completely new compressor is rather undesired as it goes hand in hand with high computational effort and does not account for long-time experience from former engine projects. Furthermore, interpretation of and confidence in newly obtained results is rather problematic, in particular related to guaranteeing reliability during operation. Hence, enforcing proven flow field characteristics for new aero engines offers several advantages concerning development time and costs.

The proposed adjustment process is typically applied manually in industrial applications where the required aerodynamic target values of the flow field, like rotor relative inlet Mach number, stator inlet Mach number, rotor/stator meridional inlet Mach number, rotor/stator static pressure rise, rotor/stator de Haller number, and rotor stage work, are usually compared graphically to the reference design in every iteration step after making some modifications and performing a flow calculation. To determine the size of the design adjustments, a lot of experience and time is required. To increase process efficiency, an automated design approach is introduced here. The basis for automated instead of manual parameter adjustment has already been discussed above. What is still missing is the driving concept and the proper objective substituting manual, graphics-based comparisons.

The cloning process and thus the comparisons have to be independent from compressor specific properties like annulus geometry, length, or number of stages. This is achieved by normalizing all geometry specific quantities and comparing them in a unified space. To receive such a geometryindependent comparison of aerodynamic quantities, radial coordinates are normalized according to Eq. (5) and stages are

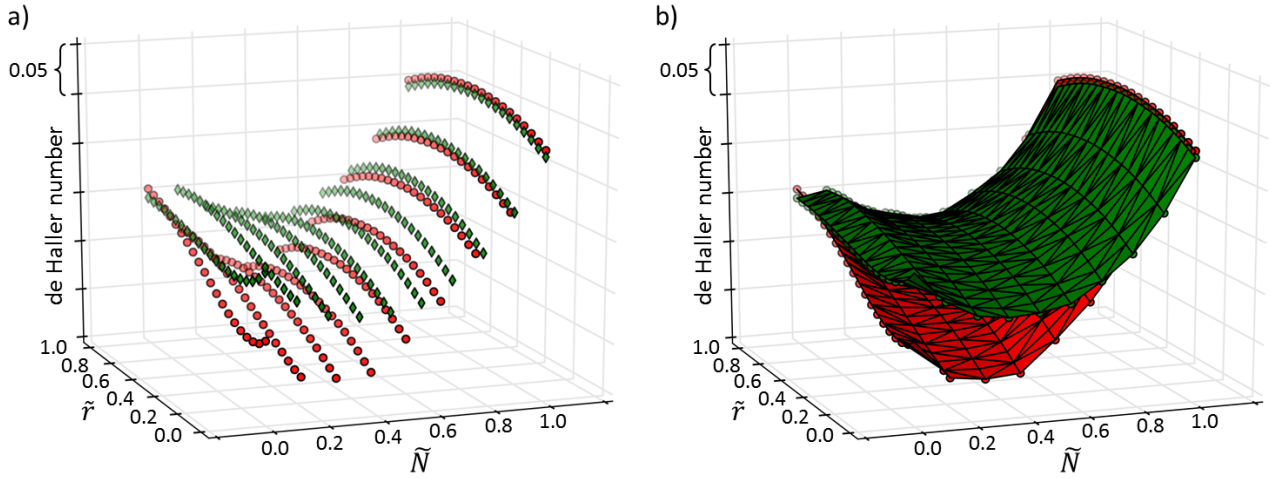

Figure 3 Comparison of a ten stage reference design (green diamonds and surface) with an alternative nine stage design (red dots and surface) for rotor de Haller number

normalized with regard to total number of stages. For the de Haller number of rotor stages, this results in a picture like Fig. 3a, where $\tilde{r}$ and $\tilde{N}$ are normalized radius and stage number, respectively. Obviously, a comparison is still problematic, if compared compressors have a different number of stages resulting in shifted curves along the $\tilde{N}$-axis. Therefore, the discrete data points are extended to surfaces as shown in Fig. 3b. An unstructured triangular grid is used where the triangles are automatically generated by using Delaunay triangulation (Su and Drysdale, 1995), and between the grid points a linear interpolation on a uniformly distributed grid of $m \times n$ measuring points is performed. These 2D measuring points can then be considered as a matrix $\boldsymbol{A} \in \mathbb{R}^{m \times n}$ with m rows and n columns. To determine the difference between a reference and a new design for a specific aerodynamic parameter, the matrices $\boldsymbol{A}_{ref}$ and $\boldsymbol{A}_{new}$ are set up and subtracted element-wise as

$$\Delta \boldsymbol{A} = \boldsymbol{A}_{new} - \boldsymbol{A}_{ref} \,. \tag{17}$$

Figure 4 shows exemplarily deviations for the rotor de Haller parameter on a 100 × 100 grid. In order to get a

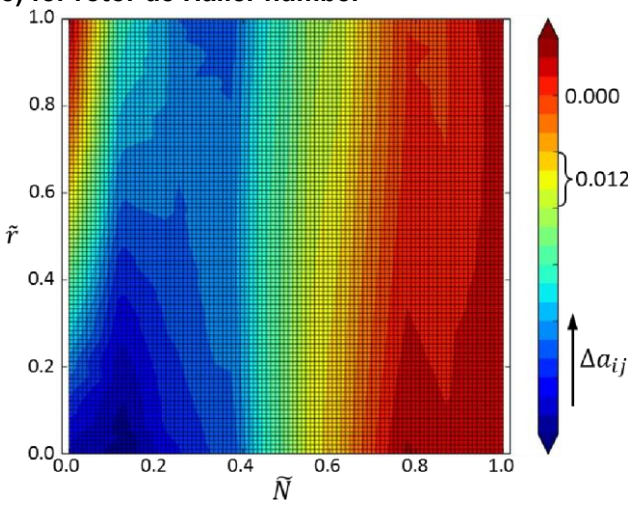

Figure 4 Deviations for rotor de Haller number on a grid with 100 × 100 cells

representative value, all errors $\Delta a_{ij} = [\Delta \boldsymbol{A}]_{ij}$ are summed up with the help of the Frobenius-norm:

$$E = \|\Delta \boldsymbol{A}\|_F = \sqrt{\sum_{i=1}^{m} \sum_{j=1}^{n} |\Delta a_{ij}|^2} \,. \tag{18}$$

Typically, multiple aerodynamic flow parameters as mentioned above have to be compared resulting in several error values E_K. For the cloning process they may be summarized as overall error

$$E_t = \sum_{k=1}^{K} E_K \tag{19}$$

to be minimized to receive a matching aerodynamic flow field. Thus, instead of the bi-criterion optimization problem (1) the new Throughflow cloning process involves only a single-criterion optimization problem:

$$\min_{\mathbf{p}_C \in P} E_t \quad where \quad P = \{\mathbf{p}_C \in \mathbb{R}^{N_C} | \mathbf{p}_C^l \le \mathbf{p}_C \le \mathbf{p}_C^u\} \tag{20}$$

where the design vector $\mathbf{p}_C$ summarizes the control points of all perturbation splines described above. The number N_C of active design parameters depends on the chosen method for perturbing radial parameter distributions.

APPLICATION RESULTS AND DISCUSSION

In order to demonstrate the functionality of the cloning strategy, the proposed cloning process is integrated in the multi-fidelity aerodynamic compressor design environment described by Hendler et al. (2017). The cascaded design philosophy described here starts with a low-fidelity compressor design process based on a 1D Meanline computation with regard to compressor efficiency η_M, where a 2D Throughflow constraint check is involved to generate proper input information for subsequent higher-fidelity processes. This process is adopted for the present case resulting in the following optimization problem to be solved prior to the 2D cloning process: max η_M *where*

$\mathbf{p}_{M \in P_M}$

$$P_M = \{\mathbf{p}_M \in \mathbb{R}^{47} | \mathbf{h}_M(\mathbf{p}_M) \le \mathbf{0}, \tag{21}$$

$$\mathbf{h}_T(\mathbf{p}_C) \le \boldsymbol{\varepsilon}_T, \mathbf{p}^l{}_M \le \mathbf{p}_M \le \mathbf{p}^u{}_M\} .$$

For finding an optimal initial compressor configuration, the preliminary design process modifies 47 different design parameters $\mathbf{p}_M$ concerning annulus shape, stage pressure ratios, axial chord lengths, and exit flow angles. The Meanline constraints $\mathbf{h}_M \le \mathbf{0}$ must be fulfilled exactly. In contrast to this, the Throughflow constraints $\mathbf{h}_T \le \boldsymbol{\varepsilon}_T$ have to be fulfilled only softly with some tolerances, because only constant radial distributions provided by Meanline are processed. The Throughflow check is necessary to find more valid compressor designs in this first design step and to compensate for some of the weaknesses of the 1D flow solver using only correlations and no radial flow information. In summary, there are 36 constraints such as limits on stage work, diffusion factor, de Haller number, Koch parameter, and inlet Mach number. Subsequently, in a general compressor design process the design information is handed over to a 2D Throughflow design process where the constraints are tightened now to be fulfilled exactly as $\mathbf{h}_T \le \mathbf{0}$ for determining a more realist radial flow field. For the new cloning process no constraints are necessary because all relevant flow information is prescribed by the reference compressor and transferred by the cloning process. Based on the solution of optimization problem (21), the cloning process (20) is started to find a design which matches the aerodynamic properties of the given reference design as close as possible. The single-objective optimization problem is solved with the Covariance Matrix Adaption Evolution Strategy (CMA-ES) (Hansen, 2006). To guarantee a fully converged solution, the number of function evaluations is set to 2250.

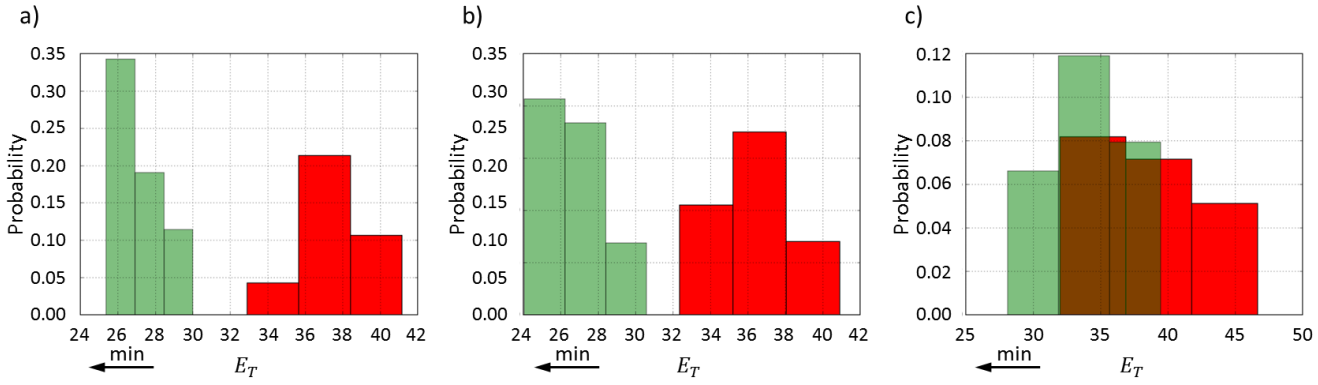

Figure 5 Total aerodynamic error for initial compressor design (red) and after subsequent cloning (green) for a) linear, b) nonlinear, and c) nonlinear without IGV modification

To apply the cloning strategy to different compressor configurations, a series of test runs is performed where the coupled processes (21) and (20) are operated by a higherlevel DoE (Design of Experiments) which modifies essential compressor settings with respect to size and positioning. For each of the two radial parameter distribution methods, linear and nonlinear, 20 compressor samples are generated, the coupled 1D/2D compressor optimization problem (21) is solved, and the aerodynamic cloning procedure

(20) is performed. Thus, for each optimal compressor design an optimized cloned design is generated. The analysis of different compressor configurations allows for a statistical assessment and the general validity of the method can be proven, which is why a different set of samples is also used for each DoE.

Figure 5 shows relative frequency plots for the total error (19) after solving problem (21) by red bars and after cloning (20) by green bars. Obviously, both radial modification strategies, linear and nonlinear, are able to improve the matching significantly, Fig. 5a and 5b. However,

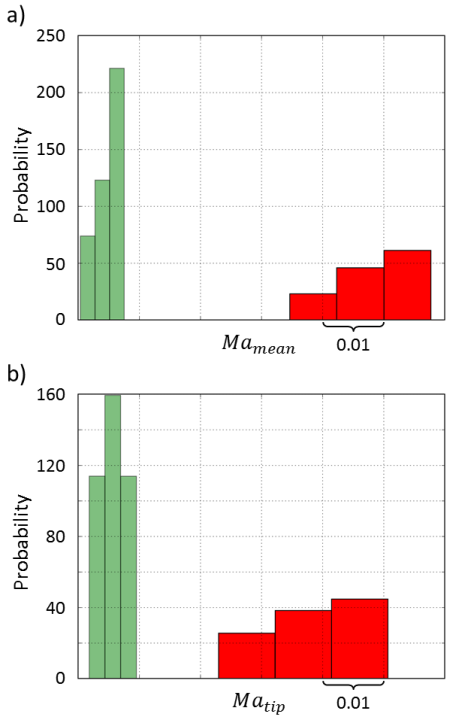

Figure 6 Frequency plots of a) mean and b) tip relative rotor inlet Mach number after optimization (21) (red) and after cloning (20) with nonlinear stator exit angle adjustment (green)

IGV modification plays an important role as Fig. 5c demonstrates by only low improvement after the cloning procedure with constant radial parameter setting.

The improved adoption of flow characteristics can also be seen in Fig. 6 where mean and tip relative rotor inlet Mach number are shown. While the aerodynamic parameter of the 1D/2D design processes are predicted particularly critical at the highly loaded aerofoil tip section, the cloning process can counteract by radially adapting blade specific parameters. The predicted velocity of the 1D/2D optimization process is extremely high which can lead to shock induced flow separation, such that an efficient or secure compressor off-design operation cannot be guaranteed. The maximum value can be reduced effectively by the cloning strategy to a similar level as for the reference compressor while other parameters are pushed to their aerodynamic limits without exceeding them. This represents the characteristics of production ready engine designs and applies in particular for the diffusion number which is slightly increased for the rotor and stator rows in the current case. In contrast, the rotor de Haller number and thus the distance to the critical lower limit found in the literature could be increased. These observations could be made for all cloned designs independently from the radial parameter distribution method.

For a better understanding of the adaption effects, different flow parameters are analysed in Fig. 7 showing exemplarily rotor relative inlet Mach number and de Haller distribution of an axially and radially normalized compressor geometry for the 1D/2D initial (above), reference (middle), and cloned (below) compressor geometry. The right pictures show the differences between initial (upper) and cloned (lower) designs with relation to the reference design, respectively. This visual comparison demonstrates the performance of the cloning process. For relevant aerodynamic flow parameters like Mach and de Haller number a very good agreement can be observed (lower right pictures, respectively).

In contrast to Rühle (2013), no dominance of the nonlinear radial distribution approach over the linear method could be found for the presented cloning approach. This means that both strategies are able to find good matching flow fields, where the linear approach may be favored due to its simplicity and lower number of design parameters in the optimization problem (20), easing its solution.

The key advantage of the cloning strategy over conventional 2D optimization approaches is the low number of function evaluations required for a fully converged solution and the absence of constraints which results in a low overall process runtime. In comparison to Pöhlmann (2015) and Rühle (2013) where convergence of a bi-criterion optimization must be ensured requiring about one day, here a fully converged solution is already available after five to seven hours without use of distributed computing, making the cloning strategy up to four times faster. A further speed up would be possible by use of distributed design evaluation.

CONCLUSIONS

The present paper examines an alternative automated approach for aerodynamic 2D Throughflow compressor design using a cloning strategy which

r

replaces the manually executed adaption process. By use of parameterization and optimization strategies, the aerodynamic characteristics of a desired reference design may be mapped on a new compressor configuration by adapting stage pressure ratios and exit flow angles. A universal approach for comparison is used to check the aerodynamic matching between adapted and reference compressor for relevant flow parameters such as de Haller number, diffusion factor, or Mach number. The sum of all squared parameter deviations from the reference design represents the design objective of the cloning approach which has to be minimized.

At the moment, no specific parameter or stage specific adjustments are part of the process. Nevertheless, all fundamental aerodynamic parameters are checked simultaneously for the whole annulus. This finally leads to an overall improvement of the aerodynamic characteristics according to the reference aerodynamic behaviour.

In comparison to other existing approaches, the proposed method is characterized by a simplified optimization problem due to (i) single- instead of multiobjective optimization and (ii) avoidance of nonlinear constraints. Both circumstances in conjunction with a lowdimensional design space reduce the computational

REFERENCES

Cumpsty N. A. (2004). Compressor Aerodynamics, Krieger, Malabar

Gräsel J., Keskin A., Swoboda M., Przewozny H. and Saxer A. (2004). A Full Parametric Model for Turbomachinery Blade Design and Optimisation, Proc. of ASME Int. Design Engineering Technical Conf. and Computers and Information in Eng. Conf., Volume 1: 30th Design Automation Conference, 907-914

Hansen N. (2006). The CMA Evolution Strategy: A Comparing Review. StudFuzz, 192, 75-102

Hendler M., Lockan M., Bestle D. and Flassig P. (2017). Component-specific Preliminary Engine Design Taking into
Account Holistic Design Aspects, Proc. of ISROMAC, Maui

Hinz M. (2012). Neue Parametrisierungsstrategien und
Methoden der Prozessbeschleunigung für die Verdichteroptimierung, PhD thesis, Brandenburg University of Technology, Shaker, Aachen

Keskin A. (2007). Process Integration and Automated Multi-Objective Optimization Supporting Aerodynamic Compressor Design, PhD thesis, Brandenburg University of Technology, Shaker, Aachen

Piegl L. and Tiller W. (1997). The NURBS Book. Monographs in visual communications, Springer, Berlin

Pöhlmann F. (2015). Optimization and Coupling Strategies for Codes of Different Fidelity to Automate an Aerodynamic Compressor Design Process, PhD thesis, Brandenburg University of Technology, Shaker, Aachen

Rühle T. (2013). Ein Beitrag zur optimalen, mehrkriteriellen Axialverdichterauslegung auf Basis der Meridianströmungsrechnung, PhD thesis, Brandenburg University of Technology, Shaker, Aachen

Rühle T. and Bestle D. (2010). Ein Verfahren zur optimalen Hochdruckverdichterauslegung auf Basis der Meridianströmungsrechnung, Proc. of DLRK 2010, DLRK2010-161166

Schönberg I. J. (1946). Contributions to the Problem of Approximation of Equidistant Data by Analytic Functions, Quart. Applied Mathematics, 4, 45-99

Su P., Drysdale R. L. S. (1995). A Comparison of Sequential Delaunay Triangulation Algorithms. Proc. of 11th Annual Symp. on Computational Geometry, 61-70, Vancouver